Acta Crystallographica Section C
Crystal Structure Communications
ISSN 0108-2701

C—H···*X* (*X* = O, N or π) interactions in benzyl carbamate

Ignasi Mata,[a]* Elies Molins,[a] Mercedes Amat,[b] Núria Llor[b] and Begoña Checa[b]

[a]Institut de Ciència de Materials de Barcelona (ICMAB–CSIC), Campus UAB, 08193 Bellaterra, Spain, and [b]Laboratory of Organic Chemistry, Faculty of Pharmacy and Institute of Biomedicine (IBUB), University of Barcelona, 08028 Barcelona, Spain
Correspondence e-mail: imata@icmab.es

Received 23 November 2011
Accepted 25 January 2012
Online 18 February 2012

The crystal packing and interaction energy of benzyl carbamate, $C_8H_9NO_2$, have been analysed in detail by the *PIXEL* method. Benzyl carbamate forms layers of hydrogen-bonded molecules, with the layers connected by weaker C—H···π interactions. According to the *PIXEL* analysis, combinations of C—H···*X* (*X* = O, N or π) interactions are comparable in energy with hydrogen bonding. These interactions are necessary for explaining the geometry and the assembly of the layers.

Comment

The carbamate group is known in biochemistry for its role in biological processes. For example, it tunes haemoglobin affinity for O_2 during physiological respiration (O'Donnell *et al.*, 1979). Carbamate derivatives present significant pharmacological activity, in some cases exhibiting potential as anticancer drugs (Bubert *et al.*, 2007). In the solid state, the carbamate group acts as both donor and acceptor in hydrogen bonding, favouring the formation of highly stable synthons. Thus, the carbamate group has been proposed in crystal engineering as a building block for hydrogen-bonded solids (Gosh *et al.*, 2006).

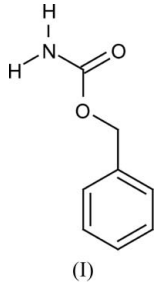

(I)

Most carbamate compounds of interest are phenyl derivatives. In the known polymorphs of one such compound, phenyl carbamate, the molecular environment is very similar around the carbamate group but very different around the phenyl ring (Wishkerman & Bernstein, 2008). In this case, polymorphism apparently arises from a different assembly of the same supramolecular synthons, suggesting that weaker interactions, such as those involving the phenyl ring, can play an important role in directing this assembly. Thus, the final molecular packing comes from the interplay of a few strong hydrogen bonds around the carbamate group with a number of weaker interactions, most of them involving the phenyl ring. In order to obtain insight into the interplay of the carbamate group and the phenyl ring in the molecular packing, the related title compound, benzyl carbamate, (I), has been crystallized, and the crystal structure analysed in detail using the *PIXEL* method (Gavezzotti, 2011).

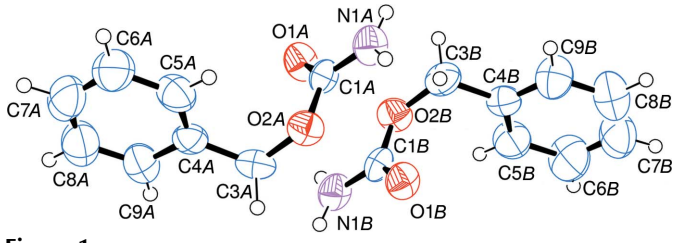

Figure 1
The molecular structure of the asymmetric unit of (I). Displacement ellipsoids are drawn at the 50% probability level.

Benzyl carbamate crystallizes in the noncentrosymmetric space group $Pca2_1$, presenting two independent molecules in the asymmetric unit, *A* and *B*, related by local symmetry centres (Fig. 1). The geometric parameters for molecules *A* and *B* are equal within three times the s.u. values. Two independent local symmetry centres are observed, situated at (0.106, 0.240, 0.748) and (0.106, 0.740, 0.748), as calculated from the average of non-H-atom pairs. The formation of a local symmetry centre close to $x = \frac{1}{8}$, $y = \frac{1}{4}$ is a common feature in this space group (Marsh *et al.*, 1998). Crystal packing in (I) takes the form of layers perpendicular to the *c* axis, with the molecules inside each layer connected by strong N—H···O hydrogen bonds and neighbouring layers connected by weak C—H···π contacts. Each layer consists of two sublayers formed exclusively of molecules *A* or molecules *B*. Interlayer contacts involve one *A* and one *B* sublayer (Fig. 2).

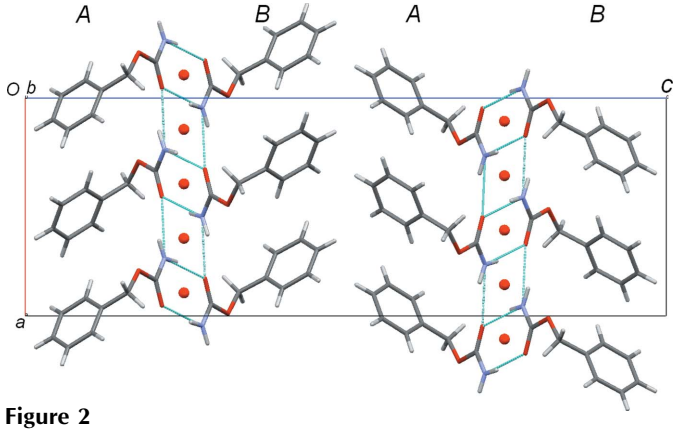

Figure 2
The molecular packing of (I), projected in the (010) plane. *A* and *B* identify the molecules in each sublayer. Large dots indicate the local symmetry centres. N—H···O interactions are indicated by dashed lines.

  doi:10.1107/S0108270112003186

The *PIXEL* method allows the calculation of the intermolecular interaction energy (E_i) inside the crystal from *ab initio* calculations on isolated molecules with the crystal geometry. *PIXEL* provides interaction energies (E_i) for pairs of molecules inside the crystal structure that take into account the polarization energy induced in the molecules by the crystal environment.

According to the calculated values of E_i, the eight lowest interaction energies correspond to pairs of molecules in the same layer, while the next three lowest interaction energies correspond to molecules in neighbouring layers. The rest of the calculated E_i values range from −2.5 to 2.0 kJ mol^{-1} and are for pairs of molecules involving two molecules that are not first neighbours in the crystal structure. As the 11 lowest E_i values account for 93% of the lattice energy, only the corresponding pairs of molecules will be considered in the following analysis. In Table 1, pairs of molecules are labelled in order of increasing E_i and identified by the most prominent intermolecular interaction, which does not mean that E_i is the energy of this particular interaction. Thus, when E_i is associated with, for example, a hydrogen bond, it should be understood as the interaction energy of the molecules connected by this hydrogen bond, and not the energy of the hydrogen bond alone. The geometry of the intermolecular interactions in Table 1 is given in Table 2.

In order to obtain an estimate of the effect of the crystal environment on the intermolecular interactions, E_i was also calculated for 11 isolated pairs of molecules with the same geometry as in the crystal structure. E_i is systematically 2–7% lower for pairs of molecules in the crystal structure, *i.e.* the crystal environment strengthens the intermolecular interactions, although its influence is small. According to this result, the crystal stability of benzyl carbamate arises from the interaction of each molecule with its primary neighbours, with little influence from the surrounding molecules.

The three lowest E_i values are for molecules connected by N—H···O hydrogen bonds, while the rest are associated with C—H···X (X = O, N or π). The qualitatively different character of these two kinds of interaction is revealed by the energy decomposition analysis provided by *PIXEL*. Thus, in strong hydrogen bonds, the most important contribution to E_i is the electrostatic energy, which is a good estimator of E_i because the sum of the other contributions (dispersion, polarization and repulsion) is approximately zero, as observed in other energy decomposition schemes based on the electron density (Abramov *et al.* 2000). In the remaining pairs of molecules, dispersion is the main contribution to E_i, while the sum of the electrostatic and polarization energies only partially compensates for the repulsion.

As shown in Fig. 2, molecule pair 1 corresponds to an $R_2^2(8)$ motif (Bernstein *et al.*, 1995) formed by two N—H···O hydrogen bonds. This supramolecular motif connects molecules *A* and *B* and is built around one of the local symmetry centres. Given the large value of E_i compared with the rest of the interaction energies, the dimer defined by $R_2^2(8)$ can be considered as the building block of the crystal structure. The next two pairs correspond to N—H···O hydrogen bonds defining two identical $C(4)$ motifs that run along [100]. Consecutive dimers along these chains are tilted, the planes defined by their $R_2^2(8)$ motifs forming an angle of 74°, calculated from the plane defined by atoms O2*A*/C1*A*/O1*A*/N1*A* and O2B^i/C1B^i/O1B^i/N1B^i [symmetry code: (i) $x, y-1, z$], and that defined by the same atoms after applying the symmetry operator ($x+\frac{1}{2}, -y, z$). Two parallel dimers along the same chain are bridged by two carbamate groups in tilted dimers, forming an $R_6^6(16)$ motif (Fig. 3). The same hydrogen-bond pattern is observed in metastable form I of phenyl carbamate (Wishkerman & Bernstein, 2008).

A feature not accounted for by hydrogen bonding is the stacked dimers along [010], with the second local symmetry center appearing between stacked dimers. The two lowest E_i values for non-hydrogen-bonded pairs of molecules (pairs 4 and 5) and the highest E_i value for an intralayer interaction (pair 8) are associated with this stacking. The short C3*A*—H3*A*1···N1A^{ii} (pair 4) and C3*B*—H3*B*2···N1B^i (pair 5) distances (all symmetry codes in this discussion are as given in Table 2) and the conformation of the carbamate groups, with an interplanar distance of 3.174 Å, calculated from the plane defined by atoms C3*A*/O2*A*/C1*A*/O1*A*/N1*A* and C3B^i/O2B^i/C1B^i/O1B^i/N1B^i, and that defined by the same atoms after applying the symmetry operator ($x, y+1, z$), with the oxo groups being almost superimposed in the direction perpendicular to the carbamate plane, suggests that these three pairs account for a complex stacking of the dimers that involves a combination of C—H···N and π–π interactions. According to *PIXEL*, this dimer stacking is similar in strength to an N—H···O hydrogen bond, playing an important role in the conformation of the layers. Thus, $R_2^2(8)$ motifs and dimer stacking define chains along [010] where each molecule in the chain is connected to its neighbours by local symmetry centres (Fig. 4). The assembly of these chains through hydrogen bonding results in layers where lines of local symmetry centres alternate with the *b*-glide plane of the crystal structure.

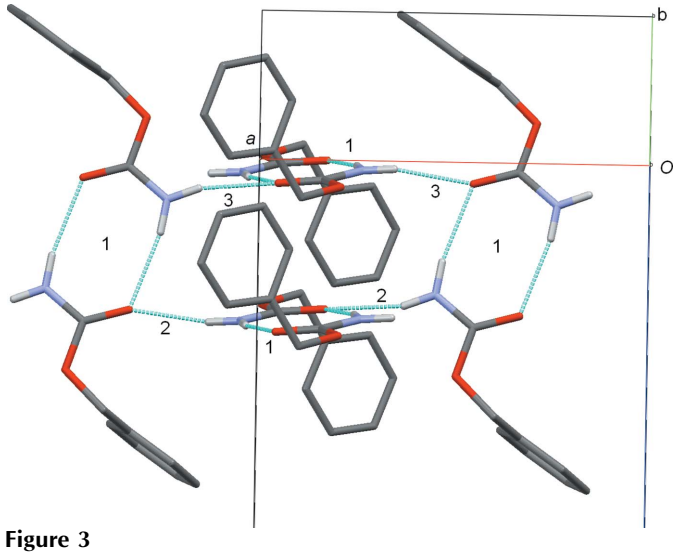

Figure 3
The hydrogen bonding in (I) (dashed lines). The numbers identify pairs of molecules in Table 1; 1 is the $R_2^2(8)$ motif, while 2 and 3 are $C(4)$. The four represented dimers form an $R_6^6(16)$ motif.

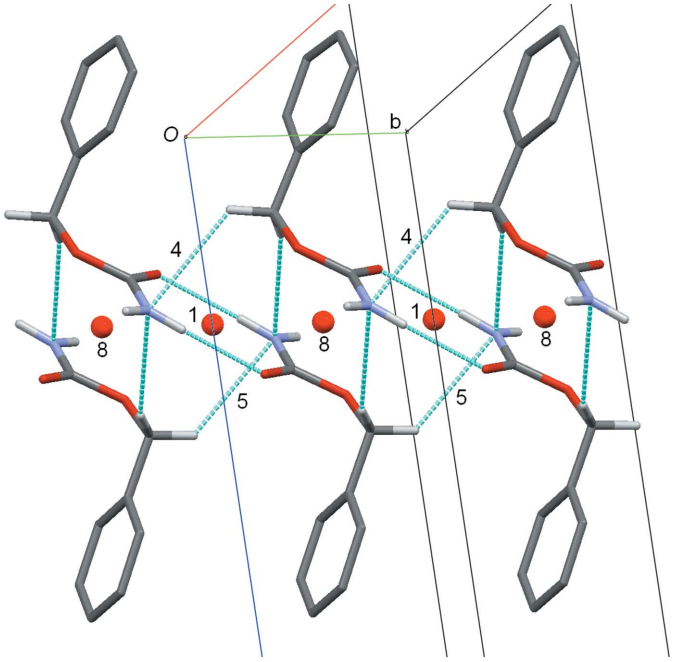

Figure 4
A view of a chain along [010]. The numbers identify pairs of molecules in Table 1. Large dots indicate local symmetry centres. N—H···O and C—H···N interactions are indicated by dashed lines.

The only significant interaction between the carbamate and phenyl groups in the *A* sublayer is C9*A*—H9*A*···O2*A*^{iv} (pair 7). The conformation of the molecule pair suggests that this interaction is reinforced by C8*A*—H8*A*···πA^{iv} (pair 7). Each molecule *A* forms two pair 7 contacts [C9*A*—H9*A*···O2*A*^{iv} and C9*A*^{viii}—H9*A*^{viii}···O2*A*; symmetry code: (viii) $x+\frac{1}{2}, -y+1, z$] and one C3*A*—H3*A*1···N1*A*^{ii} (pair 4) contact of similar E_i value with three consecutive members of the chain generated by the *C*(4) motif (Fig. 5). This is the strongest interaction bridging elements along *C*(4) and, together with the C5*A*—H5*A*···πA^{iii} contact reinforcing N1*A*—H1*A*2···O1*A*^{iii} (both in pair 3), stabilizes the tilted conformation of the molecules along the *C*(4) chains (pairs 2 and 3), to the detriment of the parallel conformation observed, for example, in the stable form II of phenyl carbamate (Wishkerman & Bernstein, 2008). The same pattern of contacts, involving pair 6, is observed in the *B* sublayer.

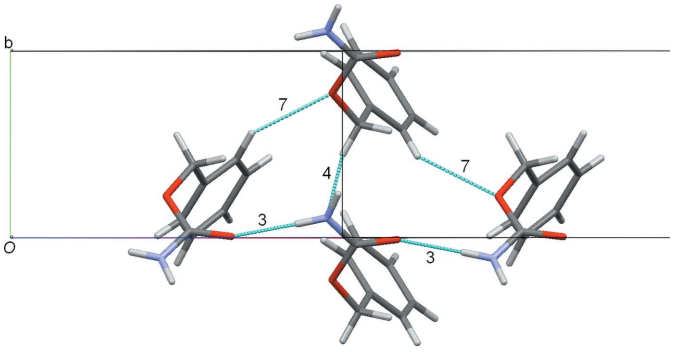

Figure 5
A view of a fragment of a *C*(4) chain with the elements bridged by C—H···O and C—H···N contacts. Numbers identify pairs of molecules in Table 1.

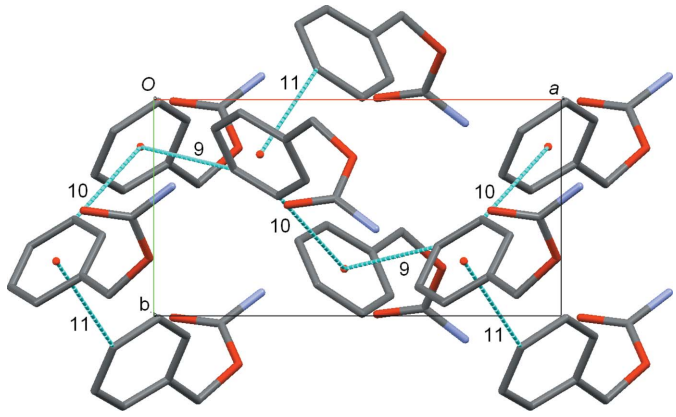

Figure 6
Detail of the interlayer assembly, projected onto the (001) plane. Selected C···*Cg* distances denoting interlayer C—H···π contacts (dashed lines) are marked. The numbers identify pairs of molecules in Table 1.

The molecule packing in a noncentrosymmetric space group arises from the assembly of layers through C—H···π contacts. These interactions can induce the formation of chiral helices arranged along the 2_1 axis, favouring crystallization in a noncentrosymmetric space group even in the case of achiral molecules (Tanaka *et al.*, 2007). The only important differences in the molecular environments of *A* and *B* concern the interlayer C—H···π contacts (Fig. 6). Thus, the geometries of H7*A*···πB^{vi} (pair 11) and H7*B*···πA^{vii} (pair 9) are quite different, with the E_i value being significantly lower for the latter. Moreover, *B* is a donor in a third C—H···π contact (pair 10) with an unconventional conformation. In this pair, the phenyl rings are almost perpendicular but the donor presents a very large offset from the centroid of the acceptor. The result deviates from the 'T' conformation usually associated with a C—H···π interaction, resembling an 'L' conformation, with a large centroid–centroid distance *CgB*···*CgA*^{ix} of 6.008 Å [symmetry code: (ix) $-x, -y+1, z+\frac{1}{2}$] and a short separation of 3.257 Å from the donor centroid *CgB* to the plane defined by the phenyl acceptor πA^{ix}. Because of this unusual conformation, this interaction can be easily missed, despite being comparable in strength with other C—H···π contacts.

In conclusion, the application of the *PIXEL* method to benzyl carbamate, (I), stresses features difficult to detect from a more conventional analysis of the structure based exclusively on geometry. Thus, the method reveals that a combination of C—H···N interactions induces a stacking that is comparable in energy with hydrogen bonding, that C—H···O and C—H···π interactions favour a tilted conformation of the molecules along hydrogen-bonded chains, and that relatively strong phenyl–phenyl interactions can take place with unusual geometries. Although hydrogen bonding is the strongest intermolecular force, there is no clear division between strong and weak interactions. Thus, even if strong hydrogen bonds are present, C—H···*X* (*X* = O, N or π) should be considered in explaining the crystal packing of benzyl carbamate.

Table 1
Pairs of molecules, interaction energies (E_i) and E_i components from *PIXEL* analysis (kJ mol^{-1}).

		E_i†	Coulombic‡	Polarization‡	Dispersion‡	Repulsion‡	Intermolecular interaction§
1	$A\cdots B^{i}$	−60.0/−58.1	−64.7	−18.4	−15.2	38.3	N1$A\cdots$O1B^{i}, N1$B\cdots$O1A^{ii}
2	$B\cdots B^{ii}$	−33.5/−32.1	−31.5	−11.6	−19.7	29.3	N1$B\cdots$O1B^{iv}, C5$B\cdots\pi B^{iv}$
3	$A\cdots A^{iii}$	−32.9/−31.9	−30.7	−11.4	−22.4	31.6	N1$A\cdots$O1A^{iii}, C5$A\cdots\pi A^{iii}$
4	$A\cdots A^{iv}$	−17.0/−16.2	−5.5	−2.4	−19.4	10.3	C3$A\cdots$N1A^{ii}
5	$B\cdots B^{i}$	−15.9/−15.2	−5.1	−2.4	−17.7	9.4	C3$B\cdots$N1B^{i}
6	$B\cdots B^{iii}$	−13.2/−12.7	−4.3	−1.3	−14.8	7.1	C9$B\cdots$O2B^{iii}, C8$B\cdots\pi B^{iii}$
7	$A\cdots A^{ii}$	−12.7/−12.1	−4.4	−1.4	−14.3	7.4	C9$A\cdots$O2A^{iv}, C8$A\cdots\pi A^{iv}$
8	$A\cdots B$	−11.1/−10.6	−1.2	−3.0	−15.4	8.6	C3$A\cdots$N1B, C3$B\cdots$N1A
9	$B\cdots A^{v}$	−7.2/−7.1	−1.4	−0.4	−7.7	2.4	C7$B\cdots\pi A^{vii}$
10	$B\cdots A^{vi}$	−5.6/−4.9	−1.3	−1.4	−10.4	7.6	C6$B\cdots\pi A^{v}$
11	$A\cdots B^{vii}$	−5.3/−5.2	−1.2	−0.3	−5.0	1.2	C7$A\cdots\pi B^{vi}$

† The first number is the interaction energy for the pair of molecules in the crystal structure and the second is for an isolated pair of molecules with crystal geometry. ‡ The components refer to E_i in the crystal structure. § πA and πB refer to π orbitals in the phenyl rings of molecules A and B, respectively. See Table 2 for all symmetry codes.

Experimental

Benzyl carbamate (300 mg) in methanol (8 ml) was heated under reflux until totally dissolved. The solution was filtered and hexane was added dropwise until the solution was slightly cloudy. Slow evaporation of the solvent at room temperature in a covered flask spiked by a hollow needle gave colourless crystals of (I). The crystals were small and of low quality, but suitable for single-crystal X-ray diffraction. Larger crystals of better quality could not be grown as crystallization experiments with other solvents were unsuccessful.

Crystal data

$C_8H_9NO_2$
M_r = 151.16
Orthorhombic, $Pca2_1$
a = 10.037 (2) Å
b = 5.330 (1) Å
c = 29.570 (4) Å
V = 1581.9 (5) Å^3
Z = 8
Mo $K\alpha$ radiation
μ = 0.09 mm^{-1}
T = 293 K
0.1 × 0.05 × 0.05 mm

Data collection

Enraf–Nonius CAD-4 diffractometer
Absorption correction: Gaussian (a grid of 8 × 8 × 8 = 512 sampling points was used); Busing & Levy (1957)
T_{min} = 0.992, T_{max} = 0.996
1472 measured reflections
1422 independent reflections
913 reflections with $I > 2\sigma(I)$
R_{int} = 0.040
2 standard reflections every 60 min
intensity decay: none

Refinement

$R[F^2 > 2\sigma(F^2)]$ = 0.076
$wR(F^2)$ = 0.233
S = 1.08
1422 reflections
199 parameters
1 restraint
H-atom parameters constrained
$\Delta\rho_{max}$ = 0.27 e Å^{-3}
$\Delta\rho_{min}$ = −0.47 e Å^{-3}

The size of the specimen crystal was small (100 × 50 × 50 µm), so the diffraction intensities were not strong. High-quality data could not be collected, converging the refinement to a large R value. H atoms were situated at calculated positions and treated as riding atoms, with Csp^3—H = 0.97 Å, Csp^2—H = 0.93 Å and N—H = 0.86 Å, and with U_{iso}(H) = 1.2U_{eq}(C,N). In the absence of significant anomalous scattering effects, Friedel pairs were not measured.

Data collection: *CAD-4 EXPRESS* (Enraf–Nonius, 1994); cell refinement: *CAD-4 EXPRESS*; data reduction: *XCAD4* (Harms & Wocadlo, 1995); program(s) used to solve structure: *SIR2004* (Burla *et al.*, 2005); program(s) used to refine structure: *SHELXL97* (Sheldrick, 2008); molecular graphics: *ORTEP-3 for Windows* (Farrugia, 1997) and *Mercury* (Macrae *et al.*, 1997); software used to prepare material for publication: *WinGX* (Farrugia, 1999).

Table 2
Geometry of intermolecular contacts (Å, °) in pairs of molecules in Table 1.

CgA and *CgB* refer to the centroids of the phenyl rings of molecules A and B, respectively.

D—H$\cdots A$	D—H	H$\cdots A$	$D\cdots A$	D—H$\cdots A$
N1A—H1A1$\cdots$O1B^{i}	0.86	2.15	2.996 (10)	169
N1B—H1B1$\cdots$O1A^{ii}	0.86	2.16	3.012 (10)	169
N1A—H1A2$\cdots$O1A^{iii}	0.86	2.08	2.903 (8)	159
N1B—H1B2$\cdots$O1B^{iv}	0.86	2.07	2.888 (8)	160
C9A—H9$A\cdots$O2A^{iv}	0.93	2.77	3.595 (12)	149
C9B—H9$B\cdots$O2B^{iii}	0.93	2.77	3.601 (13)	150
C3A—H3A1$\cdots$N1A^{ii}	0.97	2.89	3.530 (12)	124
C3B—H3B2$\cdots$N1B^{i}	0.97	2.82	3.509 (12)	128
C3A—H3A2$\cdots$N1B	0.97	3.02	3.923 (13)	155
C3B—H1B1$\cdots$N1A	0.97	3.04	3.917 (12)	152
C5A—H5$A\cdots CgA^{iii}$	0.93	3.40	4.246	152
C5B—H5$B\cdots CgB^{iv}$	0.93	3.54	4.391	154
C8A—H8$A\cdots CgA^{iv}$	0.93	3.70	4.546	152
C8B—H8$B\cdots CgB^{iii}$	0.93	3.60	4.436	151
C6B—H6$B\cdots CgA^{v}$	0.93	4.02	4.788	142
C7A—H7$A\cdots CgB^{vi}$	0.93	3.66	4.551	162
C7B—H7$B\cdots CgA^{vii}$	0.93	3.56	4.401	152

Symmetry codes: (i) $x, y-1, z$; (ii) $x, y+1, z$; (iii) $x+\frac{1}{2}, -y, z$; (iv) $x-\frac{1}{2}, -y+1, z$; (v) $-x, -y+1, z+\frac{1}{2}$; (vi) $-x, -y, z-\frac{1}{2}$; (vii) $-x+\frac{1}{2}, y, z+\frac{1}{2}$.

Financial support from the Spanish Ministry of Science and Innovation (grant Nos. CTQ2009-12520-C03-03, CTQ2009-07021/BQU and Consolider Ingenio 2010 CSD2007-00041) and from AGAUR, Generalitat de Catalunya (grant Nos. 2009-SGR-203 and 2009-SGR-1111), is gratefully acknowledged. IM thanks the Spanish National Research Council (CSIC) for a JAE-Doc fellowship financed by the European Social Fund.

Supplementary data for this paper are available from the IUCr electronic archives (Reference: UK3041). Services for accessing these data are described at the back of the journal.

References

Abramov, Y. A., Volkov, A., Wu, G. & Coppens, P. (2000). *Acta Cryst.* A**56**, 585–591.

Bernstein, J., Davis, R. E., Shimoni, L. & Chang, N.-L. (1995). *Angew. Chem. Int. Ed. Engl.* **34**, 1555–1573.

Bubert, C., Leese, M. P., Mahon, M. F., Ferrandis, E., Regis-Lydi, S., Kasprzyk, P. G., Newman, S. P., Ho, Y. T., Purohit, A., Reed, M. J. & Potter, B. V. L. (2007). *J. Med. Chem.* **50**, 4431–4443.

Burla, M. C., Caliandro, R., Camalli, M., Carrozzini, B., Cascarano, G. L., De Caro, L., Giacovazzo, C., Polidori, G. & Spagna, R. (2005). *J. Appl. Cryst.* **38**, 381–388.

Busing, W. R. & Levy, H. A. (1957). *Acta Cryst.* **10**, 180–182.

Enraf–Nonius (1994). *CAD-4 EXPRESS*. Enraf–Nonius, Delft, The Netherlands.

Farrugia, L. J. (1997). *J. Appl. Cryst.* **30**, 565.

Farrugia, L. J. (1999). *J. Appl. Cryst.* **32**, 837–838.

Gavezzotti, A. (2011). *New J. Chem.* **35**, 1360–1368.

Gosh, K., Adhikiri, S. & Fröhlich, R. (2006). *J. Mol. Struct.* **785**, 63–67.

Harms, K. & Wocadlo, S. (1995). *XCAD4*. University of Marburg, Germany.

Macrae, C. F., Bruno, I. J., Chisholm, J. A., Edgington, P. R., McCabe, P., Pidcock, E., Rodriguez-Monge, L., Taylor, R., van de Streek, J. & Wood, P. A. (2008). *J. Appl. Cryst.* **41**, 466–470.

Marsh, R. E., Schomaker, V. & Herbstein, F. H. (1998). *Acta Cryst.* B**54**, 921–924.

O'Donnell, S., Mandaro, R., Schuster, T. M. & Arnone, A. (1979). *J. Biol. Chem.* **254**, 12204–12208.

Sheldrick, G. M. (2008). *Acta Cryst.* A**64**, 112–122.

Tanaka, A., Hisaki, I., Tohnai, N. & Miyata, M. (2007). *Chem. Asian J.* **2**, 230–238.

Wishkerman, S. & Bernstein, J. (2008). *Chem. Eur. J.* **14**, 197–203.